# A COMPLETE DC AND AC ANALYSIS OF THREE PHASE CURRENT SOURCE PWM RECTIFIER USING CIRCUIT D-Q TRANSFORMATION

*Chun T. Rim*(*), *Nam S. Choi*(**), *Guk C. Cho*(**) *and Gyu H. Cho*(**)

(*) Dept. of R & D, Defence Communication Research Agency,
Seoul P.O.Box 932, 100-609, Seoul, Korea (FAX : 0342-756-1383 )
(**) Dept. of Electrical Engineering,
Korea Advanced Institute of Science and Technology (KAIST),
Kusong Dong, Yusong Gu, Taejon, 305-701, Korea (FAX : 82-42-869-3410)

**ABSTRACT:** *The recently proposed circuit D-Q transformation is used to analyze a three phase current source PWM rectifier. DC operating point and AC transfer functions are completely determined. Most features of the converter are clearly interpreted. They are (1) the output voltage can be controlled from zero to maximum, (2) the system is equivalently an ideal current source in the steady state, (3) the system can be described as linear circuits and (4) the input power factor can be arbitrarily controlled within a certain control range.*

## I. INTRODUCTION

As an excellent DC voltage source of VSI(Voltage Source Inverter) fed motor drive, the three phase current source PWM rectifier has been studied. Its numerous merits such as sinusoidal input current, power factor adjustment capability and instantaneous power flow change make it different from the conventional PCR(Phase Controlled Rectifier). Previous works are so much focused on the space vector input current control method [1][3-5] that the rectified DC voltage should be larger than some value [4-5] and nonlinear dynamic equation is generated [1][3-5].

A control method of the system which is based on the predetermined switching pattern, PWM is found in some literature [6]. And a modeling based on the equational D-Q transformation and and its application to several control methods of the DC side capacitor voltage are proposed [7]. However, so far the following important features of the ideal rectifier are seemed to be not clearly interpreted without the manipulation of complex equations:

(1) The rectified DC voltage ranges from zero to its maximum.
(2) The rectified DC part is an ideal current source in the steady state.
(3) The power factor can be controlled arbitrary within a certain control range.
(4) The system is linear when it is open-loop controlled.
(5) Full sets of the DC and linearized AC transfer functions.
(6) Open loop control as well as closed-loop control of the system is allowable.

The features are independent of PWM patterns and circuit parameters. In this paper, they are explained based on the recently proposed circuit D-Q transformation with great ease in analysis [8].

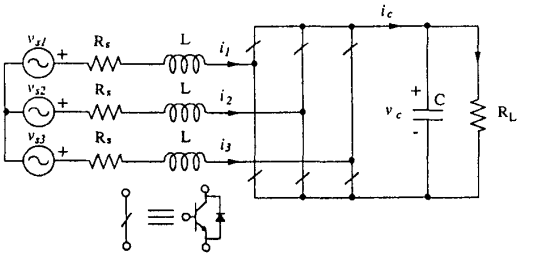


Fig. 1. Three-phase current source PWM rectifier

## II. THE CIRCUIT D-Q TRANSFORMATION OF THE SYSTEM

The system shown in Fig. 1 is a three-phase current source PWM rectifier to be modeled in this section. All circuit elements are LTI(Linear Time-Invariant). And all switches and the source

0-7803-0695-3/92 $3.00 © 1992 IEEE

voltages are ideal balanced ones. The switches operate in the CCM(Continuous Conduction Mode). And the switch pattern may be either any PWM or six-pulse control so far as its switching harmonics are not dominant. Now the switched linear time-varying system shown in Fig. 1 is to be transformed to an equivalent LTI system by the circuit D-Q transformation [8].

### A. Circuit Partitioning

The original system is too complex to analyze as a whole. So it is partitioned to several basic sub-circuits which are analyzed in advance. There are five basic sub-circuits in the switching system. They are voltage source set, resistor set, inductor set, VSI switch set and DC circuit. The rule of circuit partitioning is such that the original circuit may be composed of basic sub-circuits only. The results are shown in Fig. 2.

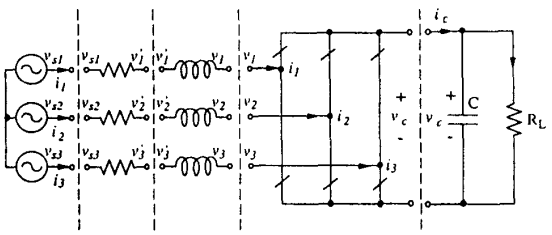

Fig. 2. Partitioned circuit

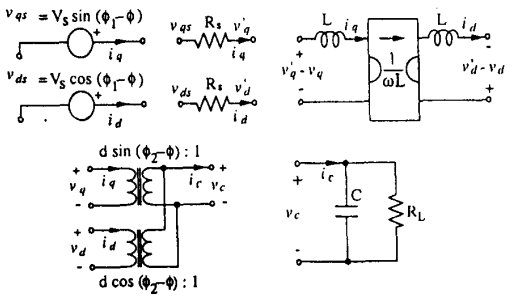

Fig. 3. D-Q transformed partitioned circuit

### B. Circuit D-Q Transformation of Sub-circuits

The rotationary circuits are now transformed to the stationary circuits. The time-varying nature of the switching system is eliminated in this way. The voltage source, switching function and power invariant D-Q transformation matrix are given as follows:

$$\mathbf{v}_{abc} = \begin{bmatrix} v_{s1} \\ v_{s2} \\ v_{s3} \end{bmatrix} = \sqrt{2/3}\ V_s \begin{bmatrix} \sin(\omega t + \phi_1) \\ \sin(\omega t - 2\pi/3 + \phi_1) \\ \sin(\omega t + 2\pi/3 + \phi_1) \end{bmatrix}, \quad (1)$$

$$\mathbf{s} = \begin{bmatrix} s_1 \\ s_2 \\ s_3 \end{bmatrix} = \sqrt{2/3}\ d \begin{bmatrix} \sin(\omega t + \phi_2) \\ \sin(\omega t - 2\pi/3 + \phi_2) \\ \sin(\omega t + 2\pi/3 + \phi_2) \end{bmatrix}, \quad (2)$$

$\mathbf{K} = \sqrt{2/3}$.

$$\begin{bmatrix} cos(\omega t + \phi) & cos(\omega t - \frac{2\pi}{3} + \phi) & cos(\omega t + \frac{2\pi}{3} + \phi) \\ sin(\omega t + \phi) & sin(\omega t - \frac{2\pi}{3} + \phi) & sin(\omega t + \frac{2\pi}{3} + \phi) \\ 1/\sqrt{2} & 1/\sqrt{2} & 1/\sqrt{2} \end{bmatrix} \quad (3)$$

$$\mathbf{K}^{-1} = \mathbf{K}^T, \quad (4)$$

where

$$\mathbf{v} = v_c \mathbf{s}, \quad \mathbf{x}_{qdo} = \mathbf{K}\mathbf{x}_{abc}. \quad (5)$$

By this transformation, the inductor set becomes a second order gyrator-coupled system and switch set becomes time-invariant transformers as well. Since all switching harmonics are assumed to be negligible, if only the fundamental component is identical, then the dynamic response is just identical regardless the PWM patterns. The result of the transformation is shown in Fig. 3.

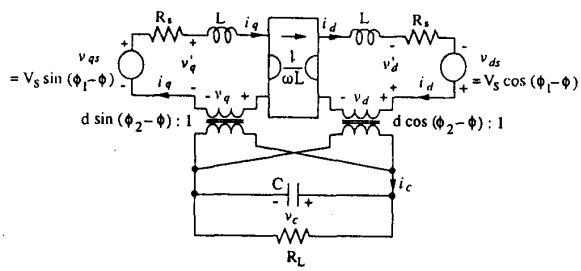

Fig. 4. Reconstructed stationary circuit

### C. Circuit Reconstruction

The rule of circuit reconstruction is to connect the adjacent related nodes where the voltage and current variables are same. The result is shown in Fig. 4. The resultant stationary circuit is composed of LTI circuit elements. Remember that previous works showed the nonlinearity of this system [1][3-5]. It can be seen that the nonlinearity does not stem from the system elements such as switches but

from the nonlinear switch control. This circuit can be directly used to find the DC operating points and the dynamic responses.

### D. Circuit Reduction

The stationary circuit shown in Fig. 4 can be simplified noticing the fact that the phase of the D-Q transform can be set to an arbitrary value. One possible selection is $\phi = \phi_1$. Then $v_q$ becomes zero as shown in Fig. 5.

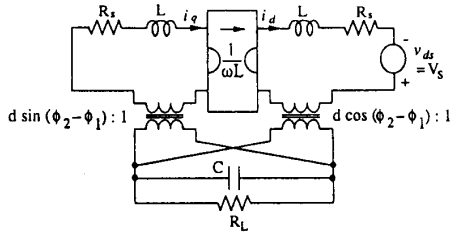


Fig. 5. Simplified circuit ($\phi = \phi_1$ case)

Another possible one is $\phi = \phi_2$. Then one of the transformers vanishes as shown in Fig. 6. It is evident that this selection simplifies the original system much more than the previous one. Remark that there is no loss of generality throughout the procedures.

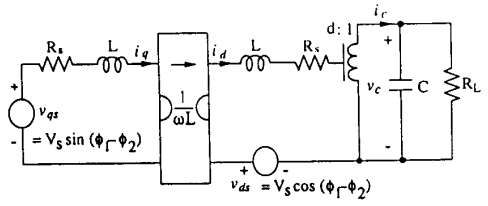


Fig. 6. Simplified circuit ($\phi = \phi_2$ case)

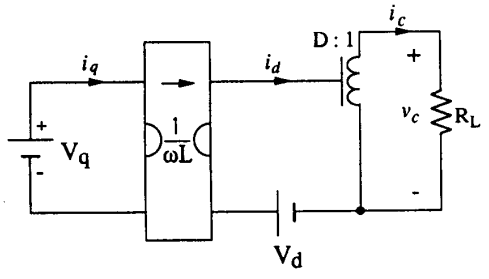


Fig. 7. DC circuit with $R_s = 0$.

## III. DC ANALYSIS

The DC analysis can be done by the steady state circuit as shown in Fig. 7 obtained from Fig. 6 by shorting the inductors and opening the capacitor. To pay our whole attention to the main features of the system, the parasitic source resistance is omitted.

### A. DC Transfer Function: $G_V$

It is found from Fig. 7 that

$$V_c = I_c R_L = I_d D R_L = \frac{V_q}{\omega L} D R_L = \frac{V_s \sin\phi_o}{\omega L} D R_L \ . \tag{6}$$

where

$$V_q = V_s \sin(\phi_1 - \phi_2) = V_s \sin\phi_o \ ,$$
$$V_d = V_s \cos(\phi_1 - \phi_2) = V_s \cos\phi_o \ . \tag{7}$$

Then the DC transfer function is found to be

$$G_V = \frac{V_c}{V_s} = \frac{\sin\phi_o}{\omega L} D R_L \ . \tag{8}$$

Note that $G_V$ ranges from zero to infinite. For given circuit parameters, the maximum DC transfer function is given by

$$G_{V,\max} = \frac{R_L}{\omega L} D_{\max} \ . \tag{9}$$

So it can be seen that for given $G_{V,\max}$ and $R_L$ the source inductor impedance should be smaller than the value determined by (9) to establish enough DC output voltage.

Fig. 8 shows the $G_V$ as a function of the phase difference between the source and inverter voltages for different modulation index D. The DC analysis based on the circuit D-Q transformation is very straightforward, so we do not have to use any cumbersome equational manipulation.

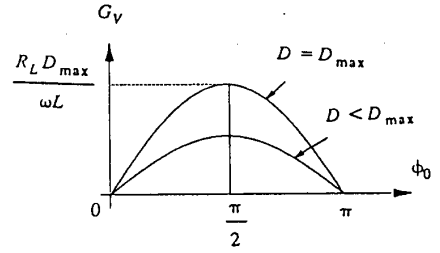


Fig. 8. The DC voltage gain.

### B. Ideal Current Source Characteristics

The rectified current $I_o$ is found from Fig. 7

and (6) as

$$I_o = I_c = \frac{V_s \sin\phi_o}{\omega L} D \ . \qquad (10)$$

Note that it is independent of the DC voltage $V_c$ or load resistor $R_L$. It is determined by circuit parameters and switching function variables only. Hence it is an ideal current source controlled by the switching function characterized by $\phi_o$ and D.

This ideal current source feature is very useful when we construct a quasi-steady state capacitor voltage controller. In case the system response is very slow it is possible to approximate the system into a first order system as shown in Fig. 9, since the capacitor is very large in practice. The maximum current is limited by the source impedance. Note the fact that negative current flow is also allowed if the switches were four-quadrant ones. Regeneration occurs instantaneously when the polarity of current is negative while the DC capacitor voltage is kept positive not in the steady state but in the transient state.

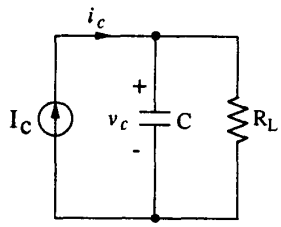


Fig. 9. Quasi-steady state output model

### C. Input Power : P, Q, PF (resistive load case)

The input real power $P$ and reactive power $Q$ are found to be

$$P = V_q I_q + V_d I_d = \frac{V_s^2}{\omega L} a \sin^2\phi_o \ , \qquad (11a)$$

$$Q = V_q I_d - V_d I_q = \frac{V_s^2}{\omega L}(1 - a \sin\phi_o \cos\phi_o) \ , \qquad (11b)$$

where

$$a = \frac{D^2 R_L}{\omega L} \ . \qquad (12)$$

Then the power factor $PF$ becomes

$$PF = \frac{P}{(P^2+Q^2)^{1/2}} = \frac{a \sin^2\phi_o}{(1 - a \sin 2\phi_o + a^2 \sin^2\phi_o)^{1/2}} \ . \qquad (13)$$

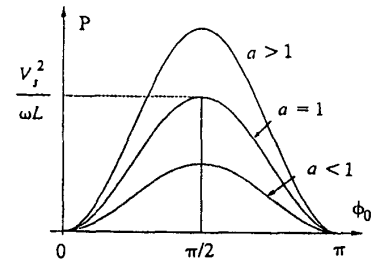


Fig. 10. Real power.

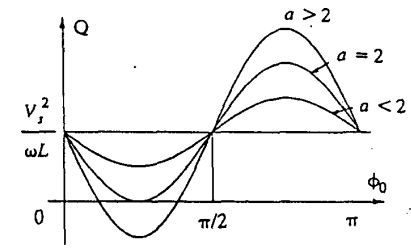


Fig. 11. Reactive power.

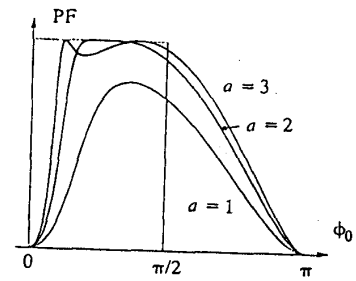


Fig. 12. Power factor.

Fig. 10, Fig. 11 and Fig. 12 show the $P$, $Q$ and $PF$ for different $a$'s, respectively. By proper selection of $a$ and $\phi_o$, the $P$ and $Q$ can be controlled as required. For the optimum operation of the system, the power factor should be at its maximum value. It can be seen from Fig. 11 that $a$ should be larger than 2 for the unity power factor. In other words power factor may not be unity when the load resistor is much low as can be seen from (13). This fact has not reported before. The unity power factor is obtained when the reactive power is zero. From (11-b) it can be seen that

$$1 - \frac{a}{2}\sin 2\phi_o = 0 \quad or \quad \phi_o = \frac{1}{2}\sin^{-1}(2/a), \ a > 2 \ . \qquad (14)$$

Under the unity power factor condition of (14) the output capacitor voltage of (6) becomes

$$V_c = \frac{V_s R_L}{\omega L} D \sin\left[\frac{1}{2}\sin^{-1}\frac{2\omega L}{D^2 R_L}\right] \approx \frac{V_s}{D}, \quad a \gg 2 . \quad (15)$$

Hence the voltage can be controlled by $D$ only. Remark that when the load resistance is much larger than the source inductor impedance, the voltage is not sensitive to the load resistance. On the other hand power factor becomes its maximum even though it is smaller than unity when the ratio of $Q$ and $P$ is minimum. This is calculated from (11) as follows:

$$PF = \frac{4a}{a^2+4}, \quad \phi_o = \sin^{-1}\frac{2}{(a^2+4)^{1/2}}, \quad a < 2 . \quad (16)$$

Fig. 13 shows the maximum power factor conditions determined by (14) and (16). There are two possible $\phi_o$'s when $a$ is larger than 2. The larger one(dotted line) can not be used in practice since the output voltage of (6) becomes too much larger than the source voltage.

### D. Input Power : P, Q, PF (No Load Case)

At no load case, the system may be a reactive power compensator. The DC voltage can be fixed to a certain predetermined value by controlling the rectified current of (10). In the steady state, real power and $PF$ are set to zeros by adjusting $\phi_o$ be zero; that is,

$$P = PF = \phi_o = 0 . \quad (17)$$

Then reactive power becomes

$$Q = \frac{V_s^2}{\omega L}(1-b), \quad b = \frac{DV_c}{V_s} . \quad (18)$$

Eq. (18) shows that the reactive power may be directly controlled by $b$ or equivalently $D$ from negative to positive as shown in Fig. 14. Considering an input side equivalent circuit (18) becomes

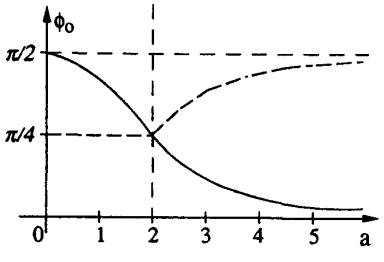


Fig. 13. Maximum power factor condition

$$Q = \begin{cases} V_s^2/\omega L_{eq} & \leftrightarrow \quad L_{eq} = \dfrac{L}{1-b}, & b<1 \\ -\omega C_{eq} V_s^2 & \leftrightarrow \quad C_{eq} = \dfrac{b-1}{\omega^2 L}, & b>1 \end{cases} \quad (19)$$

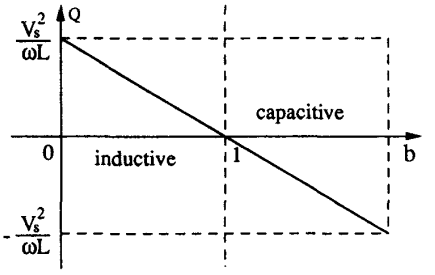


Fig. 14. Reactive power

## IV. AC ANALYSIS

In this section the specified circuit shown in Fig. 6 is analyzed. Though the equivalent circuit shown in Fig. 6 is composed of linear elements, this circuit should be perturbed since the circuit is not linear with respect to some variables. Hence the first step is to obtain a perturbed circuit from Fig. 6. There are four possible perturbation variables in the system. They are input voltage, input frequency, phase and modulation index. Among these the former two are disturbances and the latter two are control variables. Then the AC small signal perturbed circuit is drawn as shown in Fig. 15 [8]. It seems to be very complex to analyze the circuit shown in Fig. 15. It is necessary to find more simplified circuit. Fig. 16 shows this circuit where

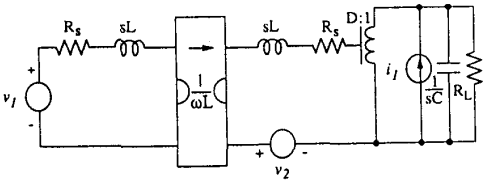


Fig. 15. AC perturbed circuit

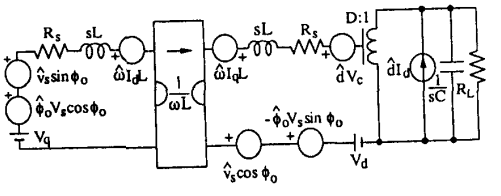


Fig. 16. Simplified circuit

sources are integrated, and DC source is eliminated. The voltage sources are

$$v_1 = \hat{v}_s \sin\phi_o + \hat{\phi}_o V_s \cos\phi_o - \hat{\omega} I_d L ,$$
$$v_2 = \hat{v}_s \cos\phi_o - \hat{\phi}_o V_s \sin\phi_o + \hat{\omega} I_q L - \hat{d} V_c , \quad (20)$$
$$i_2 = \hat{d} I_d .$$

Now the cumbersome gyrator is to be removed. Considering Norton's theorem it can be seen that

$$I_2(s) = \frac{V_1(s)}{\omega L} = \frac{V_s(s) - I_1(s)Z}{\omega L} = \frac{V_s(s)}{\omega L} - \frac{V_2(s)}{Z_{eq}} \quad (21a)$$

$$V_2(s) = \frac{Z_{eq}}{\omega L} V_s(s) - I_2(s) Z_{eq} , \quad (21b)$$

where

$$Z_{eq} = \frac{\omega L^2}{Z} . \quad (22)$$

The circuit reconstruction of (21) is Fig. 17. Applying the removal process of the gyrator and the transformer to the circuit of Fig. 16 the output voltage can be obtained as follows:

$$V_o(s) = H_1(s)V_1(s) + H_2(s)V_2(s) + H_3(s)I_1(s) \quad (23a)$$

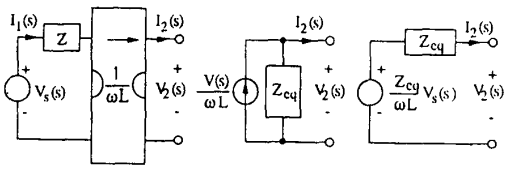


Fig. 17. The removal of gyrator

or

$$V_o(s) = H_1(s)[\hat{v}_s \sin\phi_o + \hat{\phi}_o V_s \cos\phi_o - \hat{\omega} I_d L] + H_2(s)[\hat{v}_s \cos\phi_o - \hat{\phi}_o V_s \sin\phi_o + \hat{\omega} I_q L - \hat{d} V_c] + H_3(s)[\hat{d} I_d] \quad (23b)$$

or

$$V_o(s) = G_v(s)\hat{v}_s + G_\phi(s)\hat{\phi}_o + G_\omega(s)\hat{\omega} + G_d(s)\hat{d} , \quad (23c)$$

where

$$G_v(s) = \frac{V_o(s)}{\hat{V}_s(s)} = H_1(s)\sin\phi_o + H_2(s)\cos\phi_o \quad (24a)$$

$$G_\phi(s) = \frac{V_o(s)}{\hat{\phi}_o(s)} = [H_1(s)\cos\phi_o - H_2(s)\sin\phi_o]V_s \quad (24b)$$

$$G_\omega(s) = \frac{V_o(s)}{\hat{\omega}(s)} = [-H_1(s)I_d + H_2(s)I_q]L \quad (24c)$$

$$G_d(s) = \frac{V_o(s)}{\hat{D}(s)} = -H_2(s)V_c + H_3(s)I_d \quad (24d)$$

and

$$H_1(s) = \frac{G_1(s)}{G_o(s)}, \quad H_2(s) = \frac{G_2(s)}{G_o(s)}, \quad H_3(s) = \frac{G_3(s)}{G_o(s)} . \quad (25)$$

And

$$G_o(s) = D^2 R_L (Ls + R_s) + (1 + R_L Cs)[(\omega L)^2 + (Ls + R_s)^2]$$
$$G_1(s) = \omega L D R_L$$
$$G_2(s) = (Ls + R_s) D R_L$$
$$G_3(s) = [(\omega L)^2 + (Ls + R_s)^2] R_L . \quad (26)$$

Now the four AC transfer functions are fully determined, which means the completeness of AC analysis. The transfer functions are nonlinear to the DC operating points and the system order is found to be three. The analysis is very simple because of the graphical tool, the circuit D-Q transformation.

## V. SIMULATIONAL VERIFICATIONS

Previous results are now verified by time-domain simulations. Experimental verification is not always superior to the simulational verifications since it arises unwanted discrepancy. The circuit parameters are selected as follows:

$V_s = 220[\mathrm{V}]$, $\omega = 120\pi[\mathrm{rad/sec}]$, $L = 5[\mathrm{mH}]$,
$C = 2000[\mu\mathrm{F}]$, $R_s = 1[\Omega]$, $R_L = 100[\Omega]$, $D = 1$

To verify the circuit model of Fig. 6, the step responses for $\phi_o$ are compared as shown in Fig. 18. Fig. 18(a) shows the step response of the model of Fig. 6, whereas Fig. 18(b) shows that of the original circuit of Fig. 1. It can be seen from Fig. 18 that the circuit D-Q transformed model is very exact excluding the harmonics.

## V. CONCLUSION

The rectifier has been completely analyzed throughout this paper. Several new facts are suggested and verified by a recently proposed analysis technique, the circuit D-Q transformation. The DC voltage can be controlled from zero to its maximum and the system is linear ideal current source in the steady state. The power factor is smaller than unity when $a$ is smaller than 2 whereas it becomes unity when $a$ is larger than 2. The reactive power control capability is described in detail.

Four AC small signal transfer functions are fully determined without much equational manipulations. It can be concluded that the circuit D-Q transformation is a very powerful tool in the analyses of poly-phase AC systems.

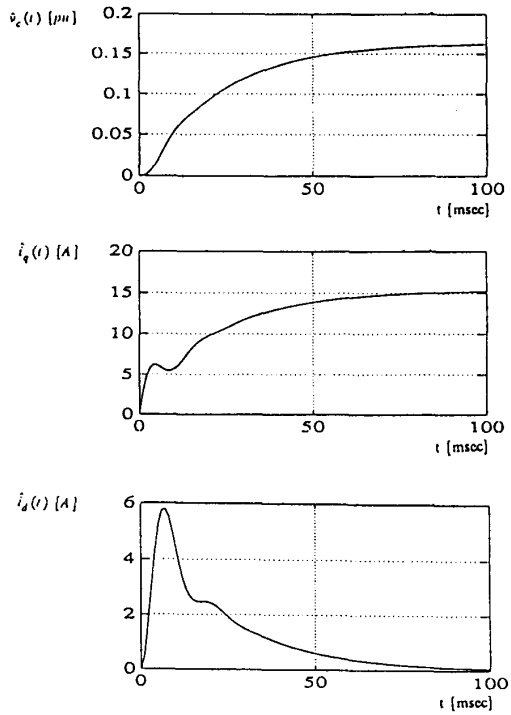


(a) Step response of the circuit model of Fig. 6.

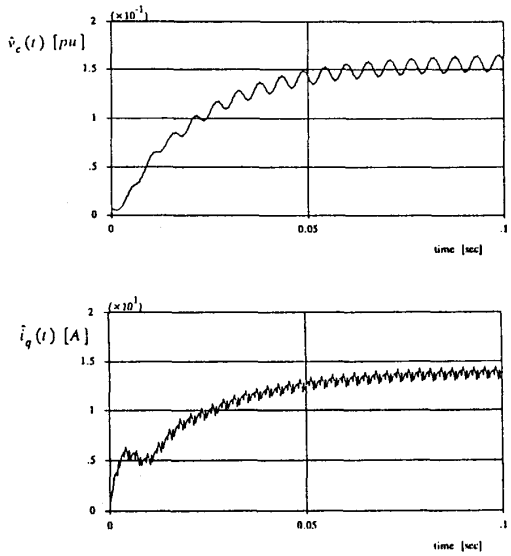


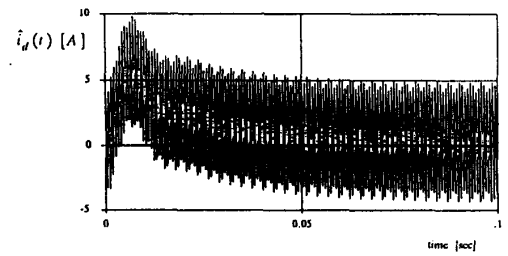


(b) Step response of the original circuit of Fig. 1.

Fig. 18. Comparison the system response of the model with that of the original circuit (input is $\hat{\phi}_o = 4u(t)[deg.]$).

## REFERENCES


[1] B. T. Ooi, J. W. Dixon, A. B. Kulkarni and M. Nishimoto, "*An integrated AC drive system using a controlled-current PWM rectifier/inverter link,*" Power Electronics, vol. PE-3, no. 1, pp. 64-71, Jan. 1988.

[2] T. A. Lipo, "*Recent progress in the development of solid-state AC motor drives,*" IEEE Trans. Power Electronics, vol. PE-3, no. 2, pp. 105-117, Apr. 1988.

[3] M. Nishimoto, J. W. Dixon, A. B. Kulkarni and B. T. Ooi, "*An integrated controlled-current PWM rectifier chopper link for sliding mode position control,*" IEEE Trans. Ind. App., vol. IA-23, no. 5, pp. 894-900, Sep./Oct. 1987.

[4] J. W. Dixon, A. B. Kulkarni, M. Nishimoto and B. T. Ooi, "*Characteristic of a controlled-current PWM rectifier-inverter link,*" IEEE Trans. Ind. App., vol. IA-23, no. 6, pp. 1022-1028, Nov./Dec. 1987.

[5] B. T. Ooi, J. C. Salmon, J. W. Dixon and A. B. Kulkarni, "*A three-phase controlled-current PWM converter with lagging power factor,*" IEEE Trans. Ind. App., vol. IA-23, no. 1, pp. 78-84, Jan./Feb. 1987.

[6] E. Wernekinck, A. Kawamura and R. Hoft, "*A high frequency AC/DC converter with unity power factor and minimum harmonic distortion,*" IEEE PESC Rec. 1987, pp. 264-270.

[7] H. Sugimoto, S. Morimoto and M. Yano, "*A high performance control method of a voltage-type PWM converter,*" IEEE PESC Rec. 1988, pp. 360-368.

[8] C. T. Rim, D. Y. Huh and G. H. Cho, "*The graphical D-Q transformation of general power switching converters,*" IEREE IAS Conf. Rec. 1988, pp. 940-945.